Data-Efficient Physics-Informed Learning to Model Synchro-Waveform Dynamics of Grid-Integrated Inverter-Based Resources

Shivanshu Tripathi[1], Hossein Mohsenzadeh Yazdi[1], Maziar Raissi[2], and Hamed Mohsenian-Rad[1]
[1]Department of Electrical and Computer Engineering, University of California, Riverside, CA, USA
[2]Department of Mathematics, University of California, Riverside, CA, USA
E-mail: {strip008, hmohs003, maziarr, hamedrad}@ucr.edu

***Abstract*— Inverter-based resources (IBRs) exhibit fast transient dynamics during network disturbances that are often not fully captured by phasor or SCADA measurements. This limitation has recently been addressed by the advent of waveform measurement units (WMUs), which provide high-resolution, time-synchronized raw voltage and current waveform samples from multiple locations in the power system. However, learning transient models from synchro-waveform measurements remains challenging owing to the scarcity of network disturbances and the complexity of the underlying nonlinear IBR dynamics. To address these challenges, we develop a data-efficient physics-informed machine learning (PIML) framework for synchro-waveform analytics that estimates the IBR terminal current response from only a small number of network disturbance signatures. Within this framework, the physics of the electrical circuit is used to compensate for limited data availability by constraining the learning process through known circuit relationships. Two cases are considered: with known and unknown circuit parameters. In the latter case, the framework jointly learns the transient dynamics of the IBRs and the circuit parameters. Case studies using WMU disturbance data across multiple sampling rates show that the proposed approach achieves consistently lower estimation error with substantially fewer training events than a purely data-driven baseline.**

Keywords: **Synchro-Waveform measurements, inverter-based resources, transient dynamics, data-driven model, network disturbances, physics-informed learning, data efficiency.**

I. Introduction

The increasing penetration of inverter-based resources (IBRs) is rapidly transforming modern power systems from synchronous to power-electronics-based, asynchronous generation. IBRs respond to grid disturbances through fast, control-driven dynamics that often involve significant sub-cycle transients. Recent reports from the North American Electric Reliability Corporation (NERC) have documented several instances of unexpected IBR behavior during grid disturbances, underscoring the need for improved modeling of IBR transient dynamics [1].

Motivated by this need, high-resolution, GPS-time-synchronized waveform measurements from waveform measurement units (WMUs) have been deployed at IBRs to model their transient dynamics at the level of raw voltage and current waveform samples. WMUs are, in essence, an extension of traditional power quality (PQ) meters and digital fault recorders (DFRs) that provide waveform samples with GPS time synchronization, either in an event-triggered format or, more recently, through continuous streaming [2].

The corresponding authors are M. Raissi and H. Mohsenian-Rad.

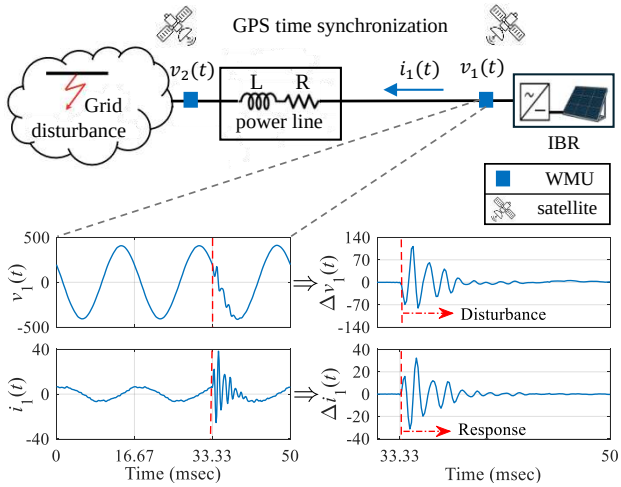

Fig. 1. Grid-connected IBR monitored by GPS time-synchronized WMUs, showing the transient voltages $v_1(t)$ and current response $i_1(t)$ following grid disturbances across line with resistance R and inductance L.

These measurements enable direct modeling of fast sub-cycle IBR dynamics using data from multiple locations [3].

Despite advancements in measurement capabilities, learning accurate IBR transient dynamic models from a *small number* of WMU-recorded disturbances remains challenging. On the one hand, *physics-only* approaches can be computationally burdensome or sensitive to uncertainty at sub-cycle time scales. On the other hand, *data-only* models require large labeled disturbance datasets that are rarely available.

To bridge this gap, this paper proposes a PIML approach. The idea is to leverage additional *grid-side* waveform measurements that can be easily collected using WMUs. These measurements are combined with IBR-site waveform measurements, allowing circuit equations to be incorporated into the PIML framework to constrain the learned dynamics; see Fig. 1 for the setup. The known circuit equations compensate for limited training data, enabling accurate modeling from a small number of WMU measurements.

***Related Work*:** The existing literature on IBR modeling can be broadly divided into two classes: *physics-based modeling* and *data-driven modeling*. Physics-based model captures electromagnetic and control dynamics [4], [5]. However, they become computationally expensive when fast timescales, such as sub-cycle transients, are involved. Their accuracy may also degrade when the underlying physics is complex, [6], and proprietary inverter controls are often inaccessible to system operators [7]. These shortcomings can

be addressed using data-driven models. Both phasor measurements [8] and waveform measurements [9], [10] have been used for this purpose. Among WMU-based methods, the approach in [9] uses regression models, while that in [10] uses Long Short-Term Memory (LSTM) models. However, these methods require waveform data from a large number of disturbances, which may take months to collect.

To reduce this data burden, we turn to PIML, which brings physical laws into the learning process [11]. In power systems, PIML has been used for optimal power flow [12], anomaly detection [13], and state estimation [14]–[16]. Closer to our setting, [7] uses a latent neural ODE with built-in inverter control structure to model proprietary grid-forming units, and [17] uses physics-informed sparse regression to learn inverter equations from hardware-in-the-loop tests. Both works rely on controlled experiments and neither estimate the surrounding circuit parameters. To our knowledge, this is the first PIML framework for synchro-waveform analytics that works with WMU-recorded disturbances and also identifies line parameters.

***Contributions*:** *First*, we propose a novel PIML approach that improves data efficiency in waveform-based IBR model learning. The proposed approach significantly improves the accuracy of learning the dynamic response of an IBR to transient disturbances, while using substantially fewer labeled instances than a purely data-driven baseline. *Second*, we simultaneously estimate the *unknown* power line parameters within the same PIML framework. *Third*, we validate our method through case studies across *different sampling rates*. The results demonstrate consistently lower estimation error and robust performance even at low sampling rates.

II. Problem Formulation

Consider again the setup in Fig. 1 with two WMUs. One WMU is installed at the IBR to measure its terminal voltage $v_1(t)$ and current $i_1(t)$. The other WMU is installed on the grid-side of the power line to measure the voltage $v_2(t)$. These measurements capture a disturbance that produces a short-duration voltage oscillation at the IBR terminal, which in turn excites a dynamic response in the inverter current.

Let $x(t) \in \{v_1(t), i_1(t), v_2(t)\}$ denote a measured waveform during a network disturbance. Rather than working directly with the raw waveforms, we use the first-order difference of the waveform samples [18, p. 151]: $\Delta x(t) \triangleq x(t) - x(t - N\Delta t), \quad t \geq t_0$, where Δt is the sampling interval, N is the number of samples per cycle, and t_0 is the onset time of the disturbance. Using $\Delta x(t)$ instead of $x(t)$ gives the disturbance signature in each waveform, removing the pre-disturbance steady-state component and captures the disturbance in $x(t)$. This also allows the learned map to generalize across operating points in the training data.

In this work, we aim to learn the relationship between the differential disturbance and the differential IBR response:

$$\Delta i_1(t) = f\big(\Delta v_1(t)\big), \quad t \geq t_0, \tag{1}$$

where $f : \mathbb{R} \to \mathbb{R}$ is an unknown nonlinear function with input $\Delta v_1(t) \in \mathbb{R}$. We use the fact that the differential waveforms satisfy the grid-side circuit equation:

$$\Delta v_2(t) = \Delta v_1(t) - R\,\Delta i_1(t) - L\,\frac{d\Delta i_1}{dt}, \quad t \geq t_0, \tag{2}$$

where R and L are resistance and inductance, respectively. Note that the physical knowledge incorporated here pertains to the IBR-grid interconnection rather than to the internal inverter dynamics, which are typically proprietary.

We collect time-synchronized measurements from p disturbance events, indexed by $k \in \{1, \ldots, p\}$. Let $\ell \in \{0, \ldots, n-1\}$ denote the sample index within an event, and define the sampling instants as $t_\ell = t_0 + \ell\Delta t$. The discrete-time measurement corresponding to a continuous-time signal is given as $x[\ell] \triangleq x(t_\ell)$. The corresponding differential samples are given by $\Delta x[\ell] = x[\ell] - x[\ell - N]$, $\ell \geq 1$. With n samples per event and p events in total, the raw measurements $x[\ell]$ collected by the WMUs are converted into differential measurements $\Delta x[\ell]$, forming the dataset:

$$\mathcal{D} := \Big\{\big\{\Delta v_{1,k}[\ell], \Delta v_{2,k}[\ell], \Delta i_{1,k}[\ell], \ell\big\}_{\ell=0}^{n-1}\Big\}_{k=1}^{p}. \tag{3}$$

We consider two variations of the above problem. First, the circuit parameters R and L are *known*, where we only need to learn the IBR current response map $f(\cdot)$. Second, the circuit parameters R and L are *unknown*, where we need to simultaneously estimate the map $f(\cdot)$ and the line parameters R and L to obtain an accurate IBR model.

III. Estimating the IBR Terminal Current Map

In this section, we present our approach to learning the IBR response map $f(\cdot)$ in (1) under both variations outlined at the end of Section II. We will then compare our PIML approach, which incorporates both the known circuit equation (2) and the differential measurements (3), against the data-driven baseline. We denote the resulting estimates of the terminal differential response by $\Delta\hat{i}_1^{\text{phy}}$ for the physics-informed model and $\Delta\hat{i}_1^{\text{data}}$ for the data-driven model.

We partition the p disturbance events into disjoint training, validation, and test sets with index sets $[\mathcal{P}_{\text{train}}, \mathcal{P}_{\text{val}}, \mathcal{P}_{\text{test}}] \subseteq \{1, \ldots, p\}$. Performance is evaluated using the mean-squared error (MSE), averaged over all samples in the test events:

$$\mathcal{L}_{\text{test}}(\Delta\hat{i}_1) := \mathbb{E}_{k\sim\mathcal{P}_{\text{test}}}\left[\frac{1}{n}\sum_{\ell=0}^{n-1}\big\|\Delta\hat{i}_1[\ell] - \Delta i_{1,k}[\ell]\big\|_2^2\right], \tag{4}$$

where $\Delta\hat{i}_1 \in \{\Delta\hat{i}_1^{\text{data}}, \Delta\hat{i}_1^{\text{phy}}\}$. We next present the learning formulation for each of the two settings:

A. Known Model Parameters

In this section, we compare the proposed physics-informed model against the data-only model trained over the same training data. Next, we describe the procedure for estimating the IBR current response for both models.

Data-only model: As a baseline, we train a neural network in the IBR training set $\{(\Delta v_{1,k}[\ell],\, \Delta i_{1,k}[\ell],\, \ell)\}_{\ell=0}^{n-1}$ for all $k \in \mathcal{P}_{\text{train}}$. Given the input pair $\{(\Delta v_{1,k}[\ell], \ell)\}$, the network predicts the terminal differential current $\Delta\hat{i}_1^{\text{data}}[\ell] \in \mathbb{R}$:

$$\Delta\hat{i}_1^{\text{data}}[\ell] = \text{NN}_{\text{data\_only}}(\Delta v_{1,k}[\ell], \ell). \tag{5}$$

The neural network parameters are learned by minimizing the empirical MSE over the training events as

$$\mathcal{L}_{\text{data}} := \mathbb{E}_{k\sim\mathcal{P}_{\text{train}}}\left[\frac{1}{n}\sum_{\ell=0}^{n-1}\left\|\Delta\hat{i}_1^{\text{data}}[\ell]-\Delta i_{1,k}[\ell]\right\|_2^2\right].$$

Physics-informed model: This model uses a neural network to predict the IBR terminal differential current response

$$\Delta\hat{i}_1^{\text{phy}}[\ell] = \text{NN}_{\text{data}}(\Delta v_{1,k}[\ell], \ell). \tag{6}$$

Training is regularized by the circuit equation (2) as

$$r[\ell] := \Delta v_{2,k}[\ell] - \Delta v_{1,k}[\ell] + R\,\Delta\hat{i}_1^{\text{phy}}[\ell] + L\,\frac{d}{dt}\Delta\hat{i}_1^{\text{phy}}[\ell],$$

where $\frac{d}{dt}\Delta\hat{i}_1^{\text{phy}}[\ell] = \frac{\Delta\hat{i}_1^{\text{phy}}[\ell]-\Delta\hat{i}_1^{\text{phy}}[\ell-1]}{\Delta t}$. The grid-side measurement $\Delta v_{2,k}[\ell]$ is used only during training to enforce circuit physics and is not required for inference. The network parameters are learned by minimizing the composite loss

$$\mathcal{L}_{\text{Phy}} := \mathbb{E}_{k\sim\mathcal{P}_{\text{train}}}\left[\frac{1}{n}\sum_{\ell=0}^{n-1}\left\|\Delta\hat{i}_1^{\text{phy}}[\ell]-\Delta i_{1,k}[\ell]\right\|_2^2+\lambda\left\|r[\ell]\right\|_2^2\right],$$

where $\lambda > 0$ is a hyperparameter chosen on the validation set. The first term fits the predicted current to the measured training data, while the second term enforces (2), acting as a physics-based regularizer.

B. Unknown Model Parameters

When the line parameters are unknown, we treat R and L as learnable scalars and estimate them jointly with the IBR current response. We parameterize $R = \phi_R(\theta_R)$, $L = \phi_L(\theta_L)$, where θ_R, θ_L are trainable scalar parameters, and $\phi_R(\cdot) = \phi_L(\cdot) = \text{softplus}(\cdot)$ enforces the physical non-negativity constraint $R, L \geq 0$. These parameters are optimized together with the neural-network weights via gradient-based training. The current predictor NN_{data} is identical to that in the known-parameter case described in Section III-A. The only modification is that the circuit residual in the physics regularization term is evaluated using the learned values of (R, L) rather than fixed ground-truth values. The training objective is the same composite loss $\mathcal{L}_{\text{Phy}}$ defined previously, so the neural network weights and the circuit parameters are updated through the same objective function. As a result, gradient-based training simultaneously estimates the IBR current response and the line parameters. In effect, the physics term both regularizes the learning problem and identifies the effective line parameters from the dataset (3).

Remark 1: At inference, the learned map $f(\cdot)$ requires only $\Delta v_1(t)$ and the index ℓ, so the deployed model operates with a single WMU at the IBR terminal. The learned map is also independent of the fault type, as it maps the voltage disturbance to the IBR response regardless of the fault type.

IV. Case Studies

We consider a single IBR connected to the grid through a single line characterized by lumped parameters (R, L), with $R = 10\ \Omega$ and $L = 0.2$ mH. The IBR terminals are monitored by GPS time-synchronized WMUs, as shown in Fig. 1. The dataset $\mathcal{D}$ defined in (3) consists of 80 disturbance events spanning different operating points[1]. We reserve 10 events for validation and 20 events for testing, and vary the number of training events over $\{3, 5, 10, 20, 30, 40, 50\}$. The validation and test sets are excluded from training and are used for hyperparameter selection λ and performance evaluation, respectively.

TABLE I

Performance comparison of data-only and physics-informed model with known R and L, and Sampling Rate of (128×60) Hz.

TrainEv	$\mathcal{L}_{\text{test}}(\Delta\hat{i}_1^{\text{data}})$	$\mathcal{L}_{\text{test}}(\Delta\hat{i}_1^{\text{phy}})$	Improvement (%)	λ
3	22.11	9.30	+57.94	0.1
5	19.06	8.85	+53.56	0.001
10	14.56	8.87	+39.03	3
20	10.83	8.85	+18.33	1
30	9.89	8.08	+18.22	0.3
40	8.69	8.23	+5.24	0.3
50	9.56	8.00	+16.29	0.1

We study both cases defined in Section II, i.e., with known and unknown R and L. In each case, we evaluate over multiple sampling rates to assess the performance of physics-informed estimator compared to the data-only baseline. In the unknown-parameter case, we additionally estimate R and L. Specifically, we consider 128, 64, and 32 samples per 60 Hz grid cycle, corresponding to

$$\Delta t \in \left\{\frac{1}{128\times60}, \frac{1}{64\times60}, \frac{1}{32\times60}\right\} \text{ sec.}$$

We consider the time horizon of each event to be 1 sec. The number of training samples depends on the time horizon, the number of training events, and the sampling rate.

A. Known Model Parameters

In this setting, the line parameters (R, L) are assumed to be known, and we compare the *data-only* and *physics-informed* estimators described in Section III-A. Both models use the same neural networks with the same architecture: two hidden layers with 32 neurons per layer and $\tanh$ activations.

Tables I-III report the performance of both models at sampling rates of (128×60) Hz, (64×60) Hz, and (32×60) Hz, respectively. Fig. 2 summarizes the average MSE of the estimated differential IBR current response across training-set sizes for each sampling rate. Across all sampling rates, the physics-informed model achieves a consistently lower MSE than the data-only baseline. Moreover, Table IV quantifies the data-efficiency gain: the physics-informed approach requires approximately 7-9 times fewer training events than the data-only model to achieve comparable or better performance.

B. Unknown Model Parameters

We adopt the same experimental setup as in Section IV-A, but now treat (R, L) as unknown and estimate them

[1]Open source code repository is made public at: https://github.com/shivanshutripath/Data-Efficient-PIML-for-IBR

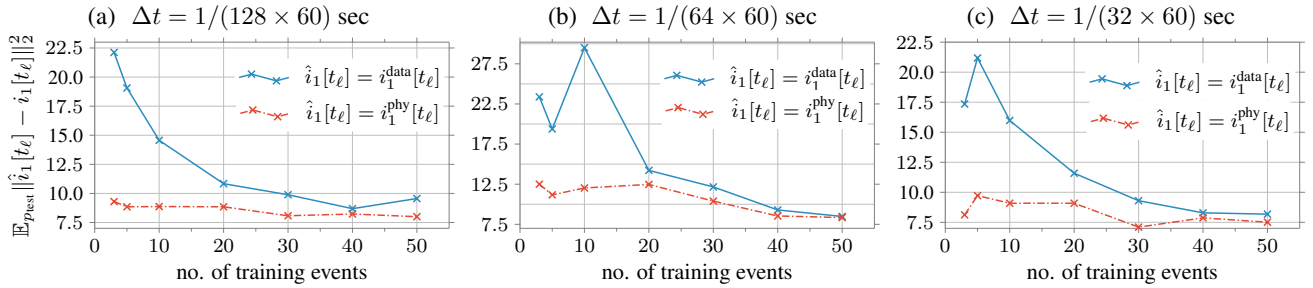

Fig. 2. The MSE for the testing data using data-only model (solid blue) and the PIML model (dashed red) for *known* circuit parameters; see Section IV-A. The PIML model achieves lower prediction error than the data-only baseline. (a)-(c) correspond to sampling rates of 128, 64, and 32 samples per cycle.

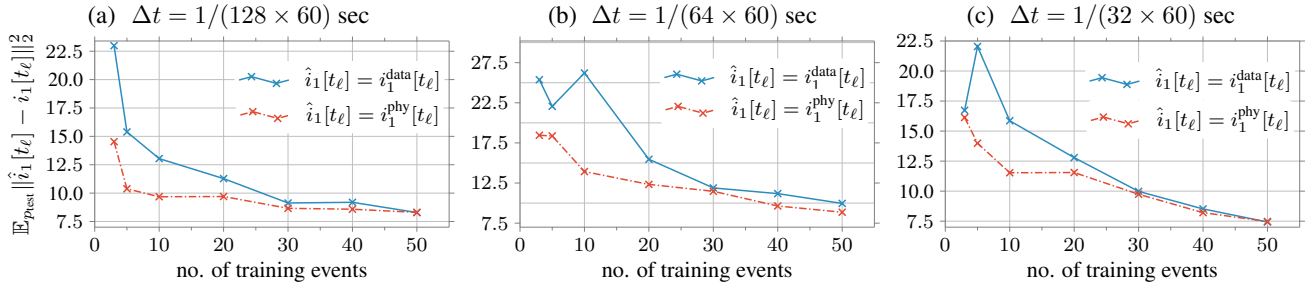

Fig. 3. The MSE for the testing data using data-only model (solid blue) and the PIML model (dashed red) for *unknown* circuit parameters; see Section IV-B. The PIML model achieves lower prediction error than the data-only baseline. (a)-(c) correspond to sampling rates of 128, 64, and 32 samples per cycle.

TABLE II

PERFORMANCE COMPARISON OF DATA-ONLY AND PHYSICS-INFORMED MODEL WITH KNOWN R AND L, AND SAMPLING RATE OF (64×60) HZ.

TrainEv	$\mathcal{L}_{\text{test}}(\Delta\hat{i}_1^{\text{data}})$	$\mathcal{L}_{\text{test}}(\Delta\hat{i}_1^{\text{phy}})$	**Improvement (%)**	λ
3	23.38	12.50	+47.65	0.1
5	19.38	11.17	+42.35	1
10	29.84	12.03	+59.67	0.0003
20	14.22	12.47	+12.30	0.003
30	12.16	10.39	+14.58	0.001
40	9.29	8.54	+8.07	0.03
50	8.48	8.34	+1.68	0.1

TABLE III

PERFORMANCE COMPARISON OF DATA-ONLY AND PHYSICS-INFORMED MODEL WITH KNOWN R AND L, AND SAMPLING RATE OF (32×60) HZ.

TrainEv	$\mathcal{L}_{\text{test}}(\Delta\hat{i}_1^{\text{data}})$	$\mathcal{L}_{\text{test}}(\Delta\hat{i}_1^{\text{phy}})$	**Improvement (%)**	λ
3	17.35	8.12	+53.20	0.1
5	21.18	9.72	+55.52	0.003
10	15.98	9.09	+36.75	0.1
20	11.59	9.09	+21.53	0.1
30	9.30	7.10	+23.69	1
40	8.29	7.87	+5.40	0.3
50	8.18	7.51	+8.14	0.01

jointly with the differential IBR current response, enabling simultaneous recovery of $\Delta\hat{i}_1(t)$ and identification of (R, L).

Tables V–VII report the MSE of the differential current response estimation and the corresponding estimates of (R, L) across sampling rates, against the ground-truth values $R = 10\ \Omega$ and $L = 0.2$ mH. Fig. 3 summarizes the average MSE versus the number of training events, and Fig. 4 shows the evolution of the learned (R, L) during training with 20 events, demonstrating stable convergence to the ground-truth values. The PIML model achieves better accuracy and higher data-efficiency than the data-only baseline, as shown in Table IV, while also identifying the circuit parameters.

TABLE IV

DATA EFFICIENCY OF PHYSICS INFORMED AND DATA-ONLY BASELINE.

Known R, L		**Unknown** R, L	
Sampling rate	**data-efficiency**	**Sampling rate**	**data-efficiency**
128	$\approx 7\times$	128	$\approx 2.34\times$
64	$\approx 9\times$	64	$\approx 5.67\times$
32	$\approx 7\times$	32	$\approx 2.34\times$

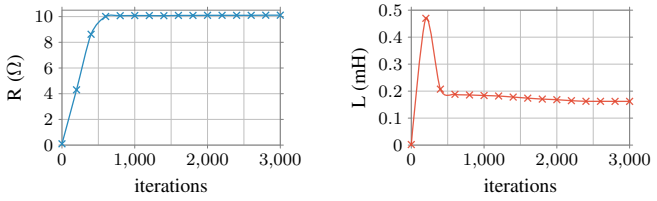

Fig. 4. The figure shows the evolution of the learned resistance R and inductance L over training iterations, using 20 training events at a sampling rate of 128×60 Hz. Both parameters are updated jointly through gradient-based optimization and converge to values close to the ground truth.

V. CONCLUSIONS AND FUTURE WORK

We proposed a data-efficient PIML framework to model the synchro-waveform dynamics of grid-integrated IBRs. The method leverages time-synchronized WMU measurements at both the IBR terminal and the grid side to embed circuit equations directly into the learning process, enabling accurate data-driven modeling with substantially fewer disturbance events than purely data-driven methods. Across multiple sampling rates, the proposed method achieves lower

TABLE V

PERFORMANCE COMPARISON OF DATA-ONLY AND PHYSICS-INFORMED MODEL WITH UNKNOWN R AND L, AND SAMPLING RATE OF (128×60) HZ.

TrainEv	$\mathcal{L}_{\textbf{test}}(\Delta\hat{i}_1^{\textbf{data}})$	$\mathcal{L}_{\textbf{test}}(\Delta\hat{i}_1^{\textbf{phy}})$	**Improvement (%)**	**Resistance (ohm)**	**Inductance (mH)**	λ
3	22.99	14.53	+36.82	9.898	0.192	0.0001
5	15.39	10.38	+32.58	9.698	0.268	1
10	13.04	9.68	+25.70	9.874	0.178	1
20	11.28	9.70	+13.93	9.906	0.169	0.00001
30	9.13	8.66	+5.17	9.750	0.220	0.3
40	9.29	8.58	+7.65	9.017	0.480	1
50	8.29	8.30	−0.06	8.852	0.548	1

TABLE VI

PERFORMANCE COMPARISON OF DATA-ONLY AND PHYSICS-INFORMED MODEL WITH UNKNOWN R AND L, AND SAMPLING RATE OF (64×60) HZ

TrainEv	$\mathcal{L}_{\textbf{test}}(\Delta\hat{i}_1^{\textbf{data}})$	$\mathcal{L}_{\textbf{test}}(\Delta\hat{i}_1^{\textbf{phy}})$	**Improvement (%)**	**Resistance (ohm)**	**Inductance (mH)**	λ
3	25.37	18.45	+27.27	9.736	0.268	0.001
5	22.06	18.37	+16.74	9.700	0.295	0.00001
10	26.21	13.93	+46.87	9.65	0.302	0.001
20	15.46	12.33	+20.25	9.293	0.403	0.3
30	11.89	11.47	+3.54	9.411	0.352	0.03
40	11.18	9.64	+13.74	8.954	0.494	0.01
50	9.96	8.86	+5.71	8.857	0.516	0.0001

TABLE VII

PERFORMANCE COMPARISON OF DATA-ONLY AND PHYSICS-INFORMED MODEL WITH UNKNOWN R AND L, AND SAMPLING RATE OF (32×60) HZ

TrainEv	$\mathcal{L}_{\textbf{test}}(\Delta\hat{i}_1^{\textbf{data}})$	$\mathcal{L}_{\textbf{test}}(\Delta\hat{i}_1^{\textbf{phy}})$	**Improvement (%)**	**Resistance (ohm)**	**Inductance (mH)**	λ
3	16.73	16.13	+3.56	8.600	0.577	0.3
5	22.04	13.99	+36.54	8.244	0.674	0.3
10	15.86	11.53	+27.32	6.867	1.062	0.3
20	12.79	11.55	+9.71	6.246	1.244	0.001
30	9.98	9.74	+2.50	6.363	1.197	0.00001
40	8.52	8.21	+3.58	6.576	1.127	0.001
50	7.43	7.47	−0.53	6.408	1.182	0.003

estimation error and robust performance. The PIML framework also supports joint estimation of unknown circuit parameters together with the IBR transient response. This capability is particularly relevant in practical settings where line parameters are uncertain or unavailable. Future work will consider more complex network settings, including multiple IBRs, inductive and capacitive components, switched systems, and three-phase unbalanced unbalanced conditions.

REFERENCES

[1] North American Electric Reliability Corporation, "Multiple Solar PV Disturbances in CAISO," NERC Report, 2022.

[2] H. Mohsenian-Rad and W. Xu, "Synchro-waveforms: A Window to the Future of Power Systems Data Analytics," *IEEE Power and Energy Magazine*, vol. 21, no. 5, pp. 68–77, 2023.

[3] H. Mohsenzadeh-Yazdi, C. Li, and H. Mohsenian-Rad, " IBR Responses During a Real-World System-Wide Disturbance: Synchro-Waveform Data Analysis, Pattern Classification, and Engineering Implications," *IEEE Trans. on Smart Grid*, pp. 1–1, 2025.

[4] P. P. Dash and M. kazerani, "Dynamic modeling and performance analysis of a grid-connected current-source inverter-based photovoltaic system," *IEEE Trans. on Sustainable Energy*, pp. 443–450, 2011.

[5] M. Ghazavi Dozein, B. C. Pal, and P. Mancarella, "Dynamics of inverter-based resources in weak distribution grids," *IEEE Trans. on Power Systems*, vol. 37, pp. 3682–3692, 2022.

[6] H. Cai, J. Xiang, and W. Wei, "Modelling, analysis and control design of a two-stage photovoltaic generation system," *IET Renewable Power Generation*, vol. 10, no. 8, pp. 1195–1203, 2016.

[7] K.-B. Kwon, S. Mukherjee, R. R. Hossain, and M. Elizondo, "Physics-informed learning of proprietary inverter models for grid dynamic studies," *arXiv preprint arXiv:2507.15259*, 2025.

[8] P. Khaledian, A. Shahsavari, and H. Mohsenian-Rad, "Event-Based Dynamic Response Modeling of Large Behind-the-Meter Solar Farms: A Data-Driven Method Based on Real-World Data," in *IEEE PES*.

[9] F. Ahmadi-Gorjayi and H. M. Rad, "Data-Driven Models for Sub-Cycle Dynamic Response of Inverter-Based Resources Using WMU Measurements," *IEEE Trans. on Smart Grid*, pp. 4125–4128, 2023.

[10] H. Mohsenzadeh-Yazdi, F. Ahmadi-Gorjayi, and H. Mohsenian-Rad, "Data-Driven Modeling of Sub-Cycle Dynamics of Inverter-Based Resources Using Real-World Synchro-Waveform Measurements," *IEEE Trans. on Power Delivery*, vol. 40, no. 4, pp. 2314–2326, 2025.

[11] M. Raissi, P. Perdikaris, and G. E. Karniadakis, "Physics-informed neural networks: A deep learning framework for solving forward and inverse problems involving nonlinear partial differential equations," *Journal of Computational Physics*, vol. 378, pp. 686–707, 2019.

[12] T. B. Lopez-Garcia and J. A. Domínguez-Navarro, "Optimal Power Flow With Physics-Informed Typed Graph Neural Networks," *IEEE Trans. on Power Systems*, vol. 40, no. 1, pp. 381–393, 2025.

[13] P. Banerjee, V. Sivaramakrishnan, and A. K. Srivastava, "Decentralized Modular Nonlinear Physics-Informed Neural Network (mnPINN) for Synchrophasor Data Anomaly Detection," *IEEE Trans. on Industry Applications*, vol. 61, no. 2, pp. 2490–2503, 2025.

[14] S. Jongh, F. Mueller, C. Cañizares, T. Leibfried, and K. Bhattacharya, "Distribution Grid State Estimation With Limited Actual and Pseudo Measurements," *IEEE Trans. on Smart Grid*, vol. 16(5), 2025.

[15] S. Falas, M. Asprou, C. Konstantinou, and M. Michael, "Robust Power System State Estimation Using Physics-Informed Neural Networks," *IEEE Trans. on Industrial Informatics*, vol. 21, pp. 8057–8067, 2025.

[16] W. Wang and N. Yu, "Estimate Three-Phase Distribution Line Parameters With Physics-Informed Graphical Learning Method," *IEEE Trans. on Power Systems*, vol. 37, no. 5, pp. 3577–3591, 2022.

[17] J. Zheng, R. Batta, Z. Liu, and X. Lu, "Discovering Unknown Inverter Governing Equations via Physics-Informed Sparse Machine Learning," *arXiv preprint arXiv:2602.16166*, 2026.

[18] H. Mohsenian-Rad, *Smart Grid Sensors: Principles and Applications*. Cambridge University Press, UK, Apr. 2022.